Effect of the electronic structure of carbon nanotubes on the selectivity of electrochemical functionalization†

Kannan Balasubramanian,*[a] Marko Burghard[a] and Klaus Kern[ab]

Received 3rd December 2007, Accepted 6th February 2008
First published as an Advance Article on the web 27th February 2008
DOI: 10.1039/b718626f

The functionalization of carbon nanotubes through electrochemical routes is gaining importance due to the high degree of control achievable and the ability to render the tubes with a variety of chemical and biological species. In this article, we report systematic investigations on the grafting of phenyl groups through diazonium coupling onto individual metallic and semiconducting carbon nanotubes both experimentally and theoretically. The results show clearly that by optimizing the electrochemical conditions it is possible to obtain a high degree of selectivity for the coupling of phenyl radicals onto metallic nanotubes. The outlined conclusions have strong implications for the design of strategies for the controlled functionalization of individual single-wall carbon nanotubes.

1. Introduction

Single-wall carbon nanotubes (SWCNTs) are emerging as prospective candidates for a variety of applications ranging from field-emission displays to scanning probe tips.[1] Their spectrum of applications can be expanded by a number of chemical functionalization approaches,[2] namely through thermally activated chemistry, photoactivated chemistry and electrochemistry. In all of these methods, the quest has been towards the ability to graft nanotubes with a desired density of functional molecules. The first two approaches, while having been successfully applied for modifying nanotubes in bulk, have a number of shortcomings including a low degree of control over the extent of modification. Electrochemistry, on the other hand, provides a convenient way to functionalize a specific subset of nanotubes (for example, those that are contacted by an electrode)[3] and offers inherent control over the extent of functionalization. By an appropriate choice of the electrochemically generated radicals, covalent or non-covalent attachment can be achieved on the surface of the contacted nanotubes.[4] In addition, electrochemical modification (ECM) serves as a generic method to attach a wide variety of chemical species ranging from metallic nanoparticles[5] to biomolecules.[6]

Initial experiments on controlled electrochemical functionalization have relied on using a certain fixed set of parameters that would yield a reproducible degree of coating.[4,5,7] Recent experiments have demonstrated that the resistance of the tubes could be monitored *in situ* while performing ECM.[8,9] Covalent functionalization of nanotubes leads to an increase in tube resistance[4,10,11] by monitoring which one can stop the grafting procedure at a specified resistance and thereby obtain a desired density of moieties on the nanotube surface. However, the effect of the electronic structure of the tube has been at the background in most of these experiments. Due to their one-dimensional nature and large level spacing, nanotube electrodes exhibit unique electrochemical characteristics as distinguished from a bulk metal or bulk semiconductor.[12] By tuning the back-gate voltage and switching the semiconducting tubes (s-SWCNTs) to the OFF state, we have demonstrated that the conductive or metallic tubes (m-SWCNTs) in a tube ensemble can be selectively functionalized.[13] This is also supported by experiments on networks of SWCNTs, which demonstrate that the amount of electrochemical charge transfer depends strongly on the electrode potential used.[14] However, recent theoretical results suggest that there exists a finite rate of charge transfer for s-SWCNTs, even in their OFF state.[12] In the following, we explore in more detail the influence of the tube's electronic structure on the functionalization extent by studying the covalent attachment of diazonium salts in a systematic manner both experimentally and theoretically on individual m- and s-SWCNTs. The experimental results demonstrate that the electrochemical attachment of phenyl radicals through diazonium coupling indeed shows a high degree of selectivity towards a specific type of nanotube. Our theoretical calculations—in addition to serving as a support for the experimental data—highlight the fact that by a judicious choice of the diazonium salt and the electrochemical parameters, it is possible to graft a certain functionality selectively on metallic tubes.

2. Experimental

Individual SWCNTs obtained from the HiPco process (Carbon Nanotechnologies Inc.) were deposited on a Si/SiO_2 substrate and contacted by AuPd–Ti electrodes with a spacing

[a] *Max–Planck–Institut fuer Festkoerperforschung, Heisenbergstrasse 1, D-70569 Stuttgart, Germany. E-mail: b.kannan@fkf.mpg.de; Fax: +49 711 6891662; Tel: +49 711 6891530*
[b] *Institut de Physique des Nanostructures, École Polytechnique Fédérale de Lausanne, CH-1015 Lausanne, Switzerland*

† Electronic supplementary information (ESI) available: *In situ* conductance profiles measured while performing ECM (Fig. S1) and calculated coupling efficiency maps in linear scale (Fig. S2). In addition, a comparison of the calculated reaction rates between the (9,0) tube and the (5,5) tube is presented. See DOI: 10.1039/b718626f

of $\sim$1.3 μm using standard procedures.[15] By measuring the back-gate dependence of conductance, the tubes were classified as metallic or semiconducting. Liquid gating experiments were performed by placing a small drop of water on top of the electrodes and covering it with a non-volatile solvent (squalane) to avoid evaporation.[15] A Ag/AgCl wire was used as the gate electrode. Such wires were prepared by pre-aging Ag wires (diameter 100 μm) for at least 4 h in a solution of $AgNO_3$ acidified with HNO_3. AgCl was then electroplated onto the wire by applying a current density of $\sim$7.5 mA cm^{-2} in 1 M HCl. The Ag/AgCl electrodes obtained in this manner showed an open-circuit potential of -75 mV ± 3 mV against a standard commercially available Ag/AgCl reference. In order to ensure a low background current through the water droplet, the electrodes were fabricated such that the contact surface area is minimal.[15] Using such a layout, resistances as high as a few GΩ could be measured without the need for a passivation layer[16,17] on top of the electrodes. The gate-dependence of conductance of a single s-SWCNT measured in this manner in a water droplet is shown in Fig. 1, where more than 3 orders of magnitude variation in conductance is clearly discernible. On the other hand, the conductance of a m-SWCNT remains almost constant. The electrical transport measurements were carried out using a home-built setup with Keithley 2400 sources, an amplifier and a Keithley 2000 multimeter. For electrochemical measurements, a Solartron 1285 potentiostat along with a Signal Recovery SR7265 lock-in amplifier was deployed.

3. Results and discussion

Since electrolyte gating and electrochemical charge transfer are intrinsically coupled,[12] the same setup can be used to perform ECM with the gate acting as a reference electrode (RE) and the nanotube acting as the working electrode (WE). For this purpose, it is only required to add an appropriate redox-active molecule to the water droplet with or without a background electrolyte. Even though the counter electrode is absent, this configuration corresponds to an electrochemical cell in a potentiostatic configuration.[18] This is due to the electrochemical currents being very low because of the small volume of the droplet and the small surface area of the electrodes.[18] Furthermore, the voltage source at the RE or the gate acts as a high-impedance instrument. In order to verify that such an arrangement indeed reproduces a potentiostatic experiment, we have also used an alternate setup where the resistance is measured through a lock-in, while the ECM is performed using an electrochemical potentiostat.[19] Both these methods have been found to deliver similar results. For all the experiments to be described below, we have used the former simpler configuration. To avoid ambiguity between the sign of the potentials used for gate voltage and electrochemical potential, we use a notation similar to that of Heller *et al.*,[12] wherein all the potentials are applied to the gate and referenced to the nanotube. Using such a convention, the cyclic voltammogram of 4-diazo-*N*,*N*-diethylaniline tetrafluoroborate (DDA) is overlaid over the gate dependence curves in Fig. 1. It is apparent that in the range of gate potentials where the DDA undergoes irreversible reduction, the m-SWCNT displays a conductance that is three orders of magnitude higher than that of the s-SWCNT.

Fig. 2 shows the conductance of a single m-SWCNT measured *in situ* while performing ECM with DDA (black curve marked DDA). As the applied gate voltage is swept to

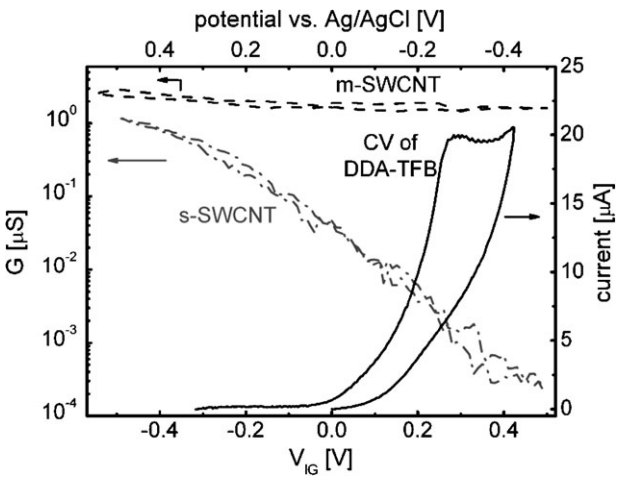

Fig. 1 Solid line: cyclic voltammogram of 10 mM 4-diazo-*N*,*N*-diethylaniline tetrafluoroborate (DDA) with 0.1 M lithium perchlorate at a gold electrode in water with Ag/AgCl as the reference. The potential at the gold electrode *versus* the reference is plotted in the top *X*-axis. Dashed and dash-dotted lines: liquid gate dependence of conductance of an individual metallic (m-SWCNT) and semiconducting (s-SWCNT) nanotube, respectively, in a water droplet. A Ag/AgCl wire is used as the gate electrode. The voltage applied to the Ag/AgCl wire with respect to the nanotube is plotted in the lower *X*-axis.

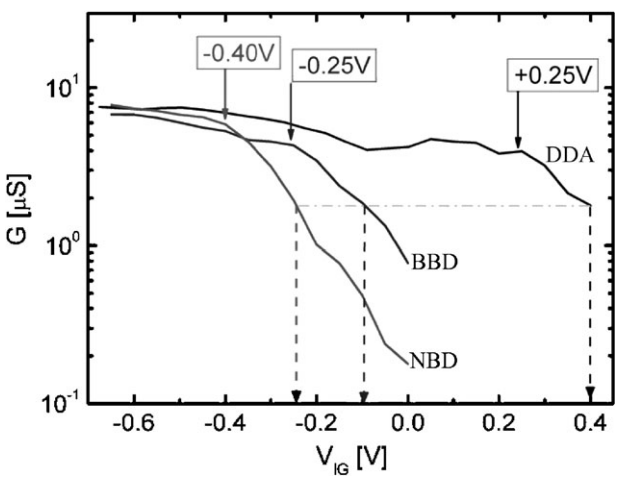

Fig. 2 Liquid gate dependence of conductance for three metallic nanotube devices monitored *in situ* while performing ECM with three different diazonium salts. A Ag/AgCl wire immersed in the droplet was used as the gate electrode. Tubes 1 (light-gray curve), 2 (dark-gray curve) and 3 (black curve) were modified, respectively, by 4-nitrobenzene diazonium tetrafluoroborate (NBD), 4-bromobenzene diazonium tetrafluoroborate (BBD) and 4-diazo-*N*,*N*-diethylaniline tetrafluoroborate (DDA). The conductance decrease of the nanotubes signifying a covalent coupling through the diazo group happens at the denoted potentials (solid filled arrows). Furthermore, at a constant overpotential with respect to these potentials, the conductances of the tubes have decreased by a constant factor (marked by dotted lines with arrowheads).

more positive values, the conductance starts decreasing at a well-defined potential (+0.25 V), in accordance with the CV in Fig. 1. In order to establish the correlation between the conductance decrease and the covalent attachment of phenyl radicals, we have also repeated the same experiment with two other single m-SWCNT devices modified, respectively, with two different diazonium salts, namely 4-nitrobenzenediazonium tetrafluoroborate (NBD) and 4-bromobenzenediazonium tetrafluoroborate (BBD). The corresponding conductance curves monitored during the attachment of the phenyl radicals are shown also in Fig. 2 (light-gray (marked NBD) and dark-gray (marked BBD) curves, respectively). It is apparent that while with BBD the conductance decrease starts at a potential of around −0.25 V, with NBD the decrease occurs at a more negative potential of around −0.4 V. This is commensurate with the reported magnitudes of the reduction peak potentials of these three salts: $V_{c:pk}^{NBD} < V_{c:pk}^{BBD} < V_{c:pk}^{DDA} = -0.45 < -0.30 < +0.30$ V,[20,21] where the convention mentioned above has been used with the potentials denoting the voltage applied to the Ag/AgCl wire with respect to the working electrode. This trend is clearly observed in the onset potentials marked by arrows in Fig. 2. Furthermore, it can be deduced that the value of conductance at a constant overpotential (as shown by the dotted lines at an overpotential of +0.15 V relating to the respective reduction potential) upon ECM is the same. The above observations, taken together with the fact that a major proportion of the applied potential falls off as a chemical potential,[12] suggests that it is possible to perform the functionalization at different levels of electronic filling by choosing an appropriate diazonium salt. Among the three salts, the reduction potential of DDA is the highest, where the difference in conductance between the m- and s-SWCNT is the largest. Thus, intuitively one would expect a sizeable difference in reactivity with m- and s-SWCNTs using DDA as the redox-active molecule. For the following, we will concentrate on the use of DDA as coupling agent and Ag/AgCl as RE to investigate the effect of electronic structure of the contacted tubes on the extent of covalent functionalization.

It is noteworthy mentioning that the modifications in Fig. 2 were performed in the absence of a background electrolyte. The background conductivity in this case is provided by the solvent (water) and the diazonium salt itself. Although this is sufficient for the transfer of appropriate potential to the nanotube-electrolyte interface, the conductance decrease is found to saturate after a few minutes. With the addition of a considerable amount of background electrolyte (lithium perchlorate), the rate of conductance decrease can be greatly improved. However, the saturation of conductance decrease is still observed (see Fig. S1 in the ESI).† While the background resistance accounts for the different rates of conductance decrease, the small volume of solution used and mass transport limitations[22] account for the saturation behaviour.[23] These observations suggest that the interface resistance at the double-layer between the tube and the solvent plays a crucial role in the effectiveness of covalent electrochemical functionalization.

Now we turn towards the effect of DDA-based ECM on the conductance of individual m- and s-SWCNTs. Fig. 3 shows the liquid gate dependence of conductance before and after performing ECM. The ECM is performed by sweeping the gate voltage up to +0.4 V for 4 cycles with the water droplet containing 10 mM DDA and 50 mM lithium perchlorate on top of the nanotube. The conductance profiles measured *in situ* while performing ECM are collected in the ESI in Fig. S1.† After the ECM, the samples were heated at 100 °C for 1 h to ensure that non-covalently attached species do not contribute to the changes in conductance through the tube. From Fig. 3, it follows that the conductance of the m-SWCNT reduces by at least an order of magnitude, whereas the conductance of the s-SWCNT remains largely unaltered. Similar curves have been obtained from other samples. If, instead of DDA, the ECM is performed with a diazonium salt whose reduction peak potential is well into the ON state of the s-SWCNT (such as with BBD), a similar decrease in conductance occurred for both types of tubes (not shown here). These observations indicate that the covalent coupling of DDA at a

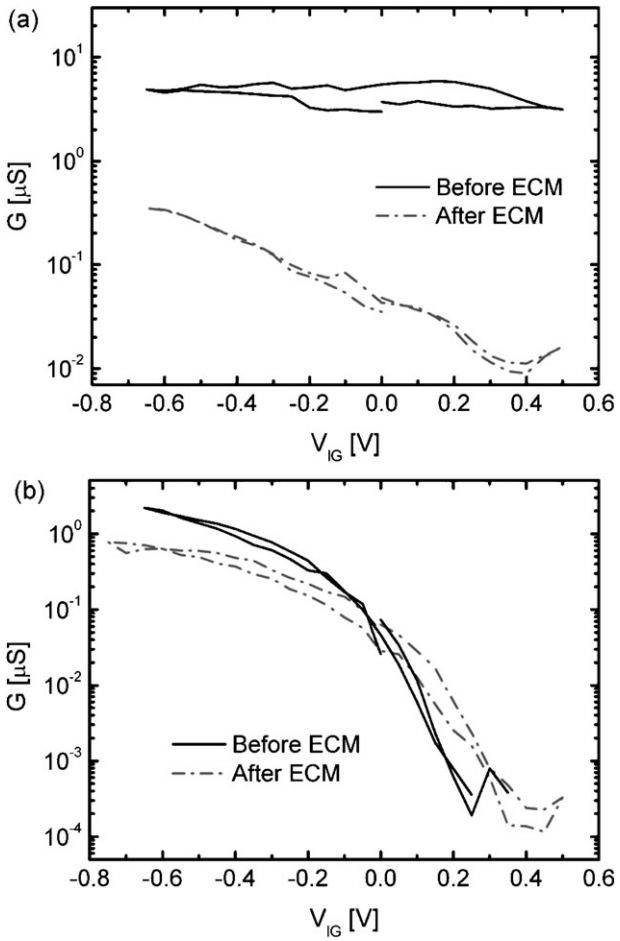

Fig. 3 Liquid gate dependence of conductance for (a) an individual metallic and (b) an individual semiconducting tube before and after ECM in a water droplet with a Ag/AgCl wire as the gate electrode. In both cases, the ECM was performed in an intermediate step by applying a maximum gate voltage of +0.4 V in a water droplet containing 10 mM DDA and 50 mM lithium perchlorate. The resistance profiles monitored *in situ* while performing the ECM are presented in the ESI (please refer to Fig. S1).† After ECM, the samples were heated to 100 °C in air for 1 h.

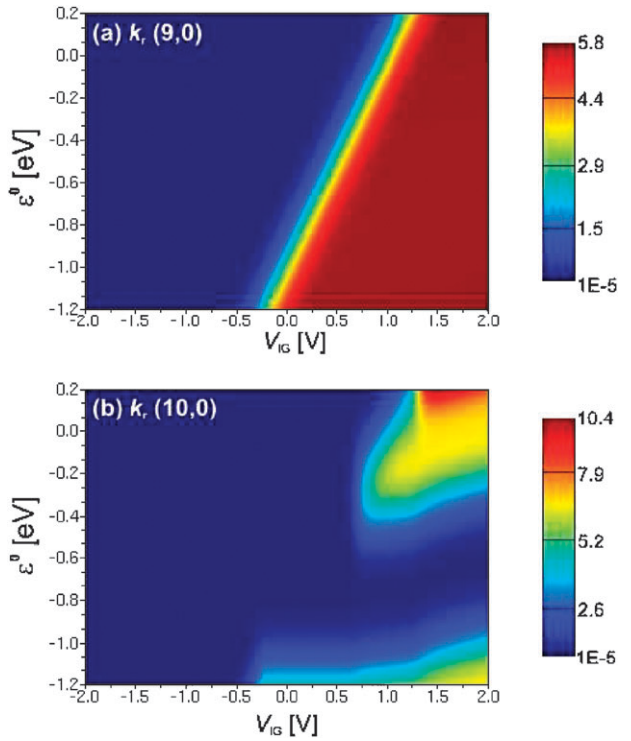

Fig. 4 Map showing the calculated reduction rates (k_r) for (a) the (9,0) m-SWCNT and (b) the (10,0) s-SWCNT plotted as a function of the applied potential (V_{IG}) and the formal potential of the redox couple (ε^0).

potential of around 0.4 V shows a high degree of selectivity towards metallic tubes.

In order to gain support for the observed selectivity in the extent of covalent functionalization for m- and s-SWCNTs, we have calculated the reduction rates at a (9,0) m- and (10,0) s-SWCNT‡ as a function of the applied gate voltage $V_{1G} = V_{appl}$ and the formal potential ε^0 of the redox couple used for performing ECM. For this purpose, we employ the Gerischer-Marcus model[24] following a procedure reported recently.[12,25] We set the half-filling energy V_{hf} to 0.2 eV, as observed in our as well as other experiments.[26] At this energy, the valence band of the nanotube is filled, while the conduction band is empty. We start by calculating the potential drop across the nanotube–electrolyte interface (V_{dl}) using the relation $V_{appl} - V_{hf} = V_{dl} + V_{ch}$, where $V_{hf} = \varepsilon_{hf}/e$. V_{ch} is the change in chemical potential, that is required to shift the Fermi level by the large energy spacing between adjacent levels in the tube. (Refer to ref. 12 for details about computing V_{ch}.) Using the calculated V_{dl}, the reduction rates at the two types of nanotubes for a redox couple with a formal potential of ε^0 is given by

$$k_r(V_{appl}, \varepsilon^0) = \nu \int W_{OX}(\varepsilon, \varepsilon^0) f(\varepsilon - eV_{appl}) \rho(\varepsilon - eV_{dl} - eV_{hf}) d\varepsilon \quad (1)$$

where $f(.)$ is the Fermi function, ρ denotes the normalized[27] electronic density of states of the (9,0) or the (10,0) tube

‡ The use of (9,0) and (10,0) tubes, respectively, as prototype metallic and semiconducting tubes for model calculations is common practice when working with the HiPco raw-material.[28]

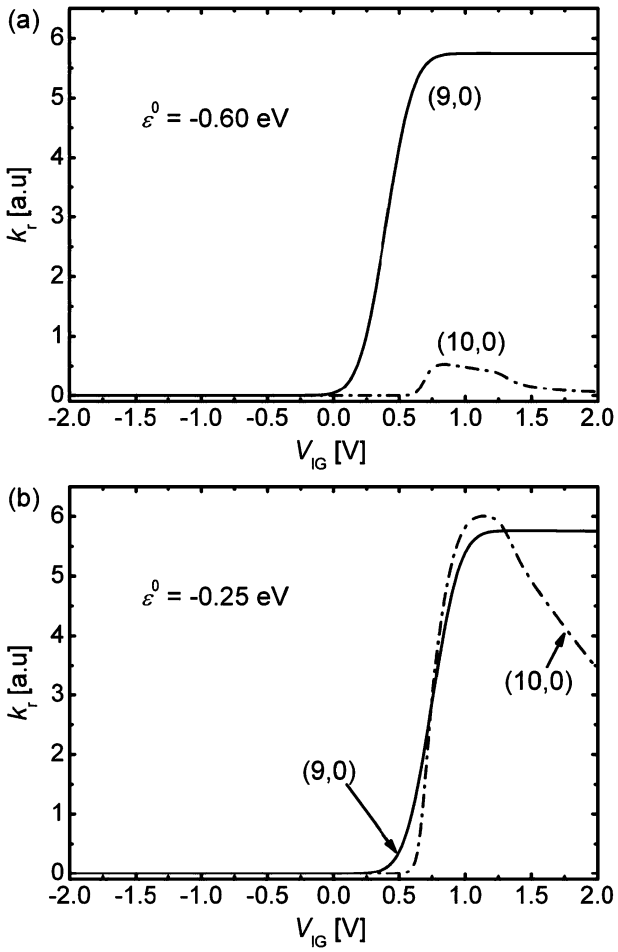

Fig. 5 Calculated k_r curves for the (9,0) m-SWCNT (solid) and the (10,0) s-SWCNT (dash-dot) for reduction with two redox couples having formal potentials of (a) −0.60 eV and (b) −0.25 eV.

(calculated using a tight-binding model[28]), and the integrand is evaluated over all energies in the range of [−10, 10] eV. W_{OX} (ε, ε^0) denotes the distribution of occupied oxidized states in solution for the specific redox couple and is modeled by a Gaussian distribution with a mean at $\varepsilon^0 + \lambda$ and a standard deviation of $\sqrt{2\lambda k_B T}$, where λ is the reorganization energy (taken as 1 eV[29]) and $k_B T$ is the thermal energy (24 meV for room temperature). ν is a prefactor which is not nanotube-specific and is taken as 1.[12,25] The reduction rates for the (9,0) and (10,0) tube calculated in this manner are presented as an image in Fig. 4a and b, respectively. It can be clearly seen from the images that there exists a certain range of ε^0 for which the reduction rate is close to zero for s-SWCNTs, whereas the m-SWCNTs have a sizeable charge transfer capability. This is further apparent from the k_r curves for the two nanotubes for two different redox couples, as shown in Fig. 5a and b. While at an ε^0 of −0.25 V, the k_r curves do not differ significantly, the k_r curves for $\varepsilon^0 = -0.6$ V indicate a comparatively higher reduction rate at the metallic tubes.

Towards quantifying the relative extent of functionalization between a m- and a s-SWCNT, we compute a metallic tube coupling efficiency Γ^{met} defined as the ratio between the

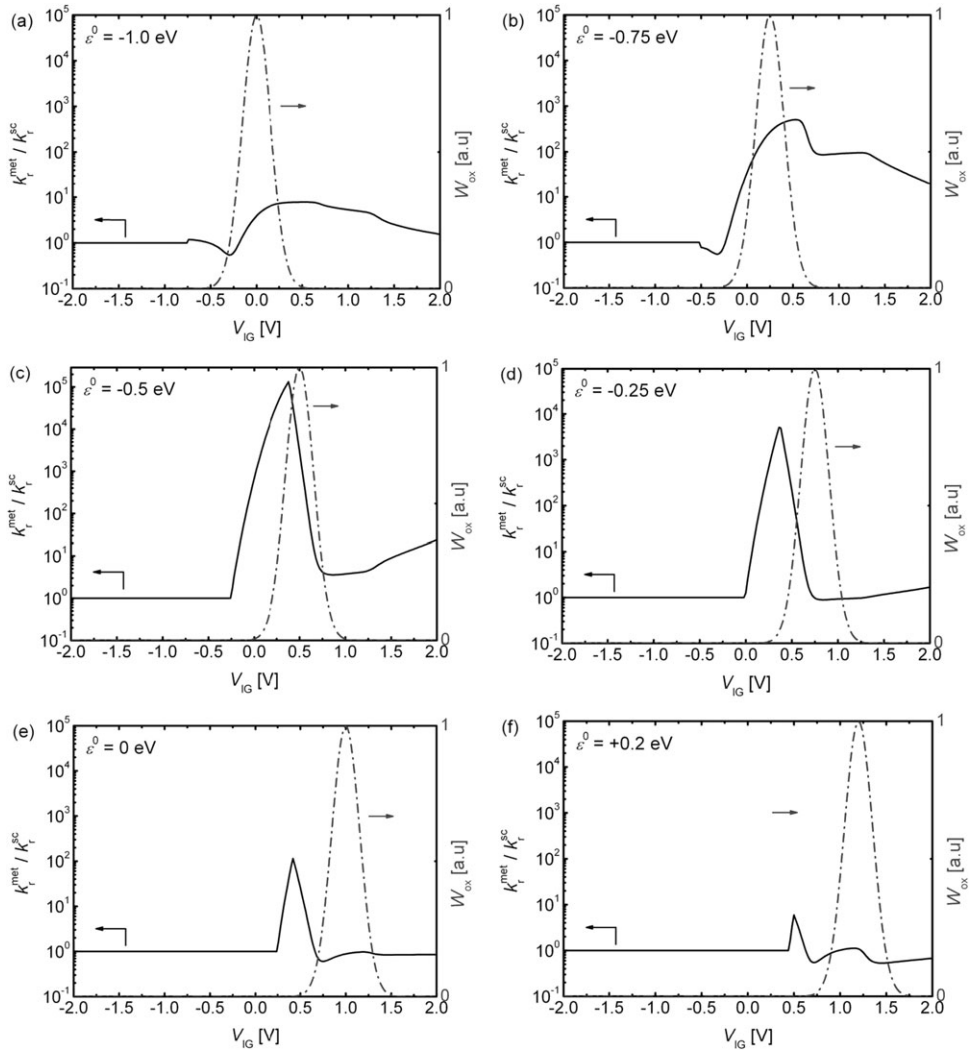

Fig. 6 (Solid lines) calculated metallic coupling efficiencies as a function of the voltage applied to the Ag/AgCl gate with redox couples of varying formal potentials (ε^0). (Dash-dotted lines) distribution of oxidized states in solution for the corresponding redox couple as a function of the gate voltage. The calculations have been carried out with $\lambda = 1$ eV and $V_{hf} = 0.2$ V.

reduction rate at a (9,0) SWCNT and the reduction rate at a (10,0) SWCNT:

$$\Gamma^{met}(V_{appl}, \varepsilon^0) = \frac{k_r^{met}(V_{appl}, \varepsilon^0)}{k_r^{sc}(V_{appl}, \varepsilon^0)} = \frac{k_r^{(9,0)}(V_{appl}, \varepsilon^0)}{k_r^{(10,0)}(V_{appl}, \varepsilon^0)} \qquad (2)$$

Such coupling efficiencies are plotted for a series of ε^0 values in Fig. 6, which demonstrates that the metallic coupling efficiency is much larger than 1 for a range of applied potentials. With an ε^0 of -0.5 eV (Fig. 6c), which roughly corresponds to the formal potential of DDA (as observed in cyclic voltammetry[18] and polarography[30]), and an applied potential of 0.32 V, the metallic coupling efficiency is maximum with the coupling of the radical being at least five orders of magnitude more effective at the (9,0) tube than at the (10,0) tube. This is in good agreement with our experimental observations of maximum selectivity of the diazo coupling through DDA when the applied potential reaches 0.4 V. The difference of 80 mV arises due to our Ag/AgCl wire having an electrode potential that is offset by -75 mV with respect to an ideal Ag/AgCl electrode. This selectivity is also visible using molecules that have a formal potential of -0.75 V (Fig. 6b), -0.25 V (Fig. 6d) and 0 V (Fig. 6e), except that the range of applied voltages where the selectivity is observable is different. Furthermore, for all curves there exists a small voltage range where the metallic coupling efficiency is smaller than 1, signifying a slightly increased reactivity on s-SWCNTs. Finally, with ε^0 values of -1 eV and 0.2 eV (Fig. 6a and f), the modulation in the coupling efficiency is less than an order of magnitude. This again agrees well with the low degree of selectivity observed in our ECM experiments with BBD (whose formal potential is close to -1 eV).

There are several factors that are to be kept in mind while interpreting the above-mentioned results. First, various aspects related to the redox-couple such as dipole moment, steric hindrances, *etc.*, have not been considered in the calculations. The reactivity and, hence, the selectivity will depend on such factors.[31] Secondly, as mentioned above, the background conductance of the electrolyte that occurs in series with the electrochemical double layer plays an important

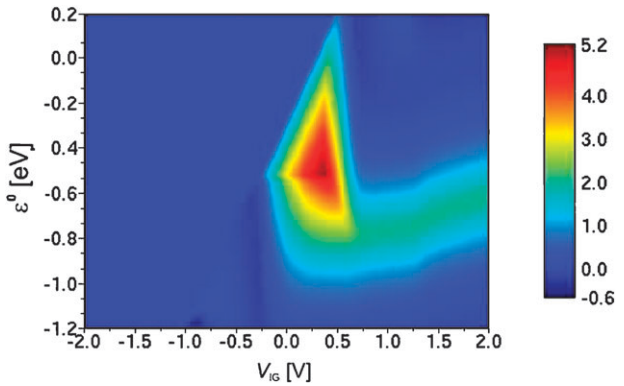

Fig. 7 Map showing metallic coupling efficiency plotted in log scale as a function of the formal potential (ε^0) and the applied gate voltage (V_{IG}) at a Ag/AgCl wire. The metallic coupling efficiency is defined as the ratio of reduction rate at a metallic (9,0) tube to the reduction rate at a semiconducting (10,0) tube. In the image, 0 corresponds to the situation where the reduction rates at both tubes are equal. Positive values denote a relatively preferred coupling to the (9,0) tube, while negative values signify a higher reduction rate at the semiconducting (10,0) tube. A linear scale plot of the same map and its inverse can be found in the ESI (see Fig. S2).†

role on the efficiency of molecular grafting. Another important circuit component is the contact resistance at the metal-electrode/nanotube interface which also occurs in series with the double layer. While for m-SWCNTs this makes a negligible contribution, for s-SWCNTs in the OFF state it can be quite high. If this is incorporated into the calculations, this would improve the coupling efficiency at an m-SWCNT to a value that is higher than that calculated in the above simulations. Furthermore, it is pertinent to note that the calculations assume that the conduction band of a s-SWCNT is directly accessible. However, this is not the case in reality due to the large Schottky barrier for electron injection into the contacted nanotube.[32,33] Again this component would increase the coupling efficiency of the diazonium salts towards m-SWCNTs. From the foregoing discussions, it can be concluded that the calculated metallic coupling efficiencies in the range of 3 to 5 orders of magnitude are sufficient to ensure a selective coating on metallic nanotubes. Needless to say, this is only valid for a specific set of electrochemical parameters. For the sake of comparison, we have performed a similar analysis also for the (5,5) arm-chair tube, which is metallic. From the results of the calculations (as shown in Fig. S3 to S6 in the ESI),† we observe that there is hardly a difference in the reaction rates among different metallic tubes.

Fig. 7 displays a map of the metallic coupling efficiency (in log scale) against the formal potential and the applied voltage. This map serves as a guide to identify the appropriate set of electrochemical parameters to maximize selectivity. Specifically, to obtain a highly selective coupling to the metallic SWCNT, one would choose an ε^0 close to -0.55 eV and a V_{appl} of around 0.3 V, as can be inferred from the bright spots in the map. Furthermore, if a rather equivalent degree of DDA-derived coating on both m- as well as s-SWCNTs is desired, a potential larger than 0.4 V should be used.

4. Conclusion

In conclusion, we have investigated the effect of nanotube electronic structure on the extent of covalent electrochemical functionalization both experimentally and theoretically. The functionalization has been carried out using diazonium salts with differing phenyl substituents. By observing the changes in conductance of individually contacted nanotubes we have shown that at certain potentials the metallic nanotubes are modified much more strongly than their semiconducting counterparts. Theoretical simulations based on the Gerischer-Marcus model support this observation. With the ongoing progress in reducing the chirality distribution of the produced nanotubes,[34] it will be possible to graft a certain functionality in a desired density on a tube in a very controlled manner.

Acknowledgements

This work was supported by the Deutsche Forschungsgemeinschaft within the framework of the priority program SPP1121.

References

1 G. Cuniberti, G. Fagas and K. Richter, *Introducing Molecular Electronics (Lecture Notes in Physics vol. 680)*, Springer Verlag, Berlin-Heidelberg, 2005.
2 M. Burghard, *Surf. Sci. Rep.*, 2005, **58**, 1.
3 S. E. Kooi, U. Schlecht, M. Burghard and K. Kern, *Angew. Chem., Int. Ed.*, 2002, **41**, 1353.
4 K. Balasubramanian, M. Friederich, C. Jiang, Y. Fan, A. Mews, M. Burghard and K. Kern, *Adv. Mater.*, 2003, **15**, 1515.
5 T. M. Day, P. R. Unwin, N. R. Wilson and J. V. Macpherson, *J. Am. Chem. Soc.*, 2005, **127**, 10639.
6 K. Balasubramanian and M. Burghard, *Anal. Bioanal. Chem.*, 2006, **385**, 452.
7 U. Schlecht, K. Balasubramanian, M. Burghard and K. Kern, *Appl. Surf. Sci.*, 2007, **253**, 8394.
8 J. Mannik, B. R. Goldsmith, A. Kane and P. G. Collins, *Phys. Rev. Lett.*, 2006, **97**, 016601.
9 B. R. Goldsmith, J. G. Coroneus, V. R. Khalap, A. A. Kane, G. A. Weiss and P. G. Collins, *Science*, 2007, **315**, 77.
10 C. Wang, Q. Cao, T. Ozel, A. Gaur, J. A. Rogers and M. Shim, *J. Am. Chem. Soc.*, 2005, **127**, 11460.
11 J. Cabana and R. Martel, *J. Am. Chem. Soc.*, 2007, **129**, 2244.
12 I. Heller, J. Kong, K. A. Williams, C. Dekker and S. G. Lemay, *J. Am. Chem. Soc.*, 2006, **128**, 7353.
13 K. Balasubramanian, R. Sordan, M. Burghard and K. Kern, *Nano Lett.*, 2004, **4**, 827.
14 T. M. Day, N. R. Wilson and J. V. Macpherson, *J. Am. Chem. Soc.*, 2004, **126**, 16724.
15 A. Maroto, K. Balasubramanian, M. Burghard and K. Kern, *ChemPhysChem*, 2007, **8**, 220.
16 M. P. Lu, C.-Y. Hsiao, P.-Y. Lo, J.-H. Wei, Y.-S. Yang and M.-J. Chen, *Appl. Phys. Lett.*, 2006, **88**, 053114.
17 M. Burghard, A. Maroto, K. Balasubramanian, T. Assmus, A. Forment-Aliaga, E. J. H. Lee, R. T. Weitz, M. Scolari, F. Nan, A. Mews and K. Kern, *Phys. Status Solidi B*, 2007, **244**, 4021.
18 J. Wang, *Analytical Electrochemistry*, Wiley-VCH, Weinheim, 2000, ch. 2.
19 M. M. Deshmukh, A. L. Prieto, Q. Gu and H. Park, *Nano Lett.*, 2003, **3**, 1383.
20 P. Allongue, M. Delamar, B. Desbat, O. Fagebaume, R. Hitmi, J. Pinson and J.-M. Saveant, *J. Am. Chem. Soc.*, 1997, **119**, 201.
21 S. Baranton and D. Belanger, *J. Phys. Chem. B*, 2005, **109**, 24401.
22 P. E. Sheehan and L. J. Whitman, *Nano Lett.*, 2005, **5**, 803.
23 A. Laforgue, T. Addou and D. Belanger, *Langmuir*, 2005, **21**, 6855.

24 A. J. Bard and L. R. Faulkner, *Electrochemical Methods Fundamentalsand Applications*, John Wiley and Sons, New York, 2001, section 3.6.3, pp. 124–130.
25 N. Nair, W.-J. Kim, M. L. Usrey and M. S. Strano, *J. Am. Chem. Soc*., 2007, **129**, 3946.
26 S. Rosenblatt, Y. Yaish, J. Park, J. Gore, V. Sazonova and P. L. McEuen, *Nano Lett*., 2002, **2**, 869.
27 N. Nemec and G. Cuniberti, *Phys. Rev. B*, 2006, **74**, 165411.
28 R. Saito, G. Dresselhaus and M. S. Dresselhaus, *Physical Properties of Carbon Nanotubes*, Imperial College Press, London, 1998.
29 W. J. Albery, *Annu. Rev. Phys. Chem*., 1980, **31**, 227.
30 R. M. Elofson and F. F. Gadallah, *J. Org. Chem*., 1968, **34**, 854.
31 P. Hartig, Th. Dittrich and J. Rappich, *J. Electroanal. Chem*., 2002, **524–525**, 120.
32 Y. F. Chen and M. S. Fuhrer, *Nano Lett*., 2006, **6**, 2158.
33 E. J. H. Lee, K. Balasubramanian, J. Dorfmueller, R. Vogelgesang, N. Fu, A. Mews, M. Burghard and K. Kern, *Small*, 2007, **3**, 2038.
34 B. Wang, C. H. P. Poa, L. Wei, L.-J. Li, Y. Yang and Y. Chen, *J. Am. Chem. Soc*., 2007, **129**, 9014.

